Cite this: *Dalton Trans.*, 2021, **50**, 5759Received 4th March 2021,
Accepted 26th March 2021

DOI: 10.1039/d1dt00726b

rsc.li/dalton

Water-stable lanthanide–organic macrocycles from a 1,2,4-triazole-based chelate for enantiomeric excess detection and pesticide sensing†

Kai Cheng,^{a,b} Qi-Xia Bai,^c Shao-Jun Hu,^{a,b} Xiao-Qing Guo,^{a,b} Li-Peng Zhou,^{id}^a Ting-Zheng Xie^{id}^c and Qing-Fu Sun^{id}^{*a,b}

Water-stable anionic Ln₂L₂-type (Ln = La^{III} and Eu^{III}) lanthanide–organic macrocycles have been constructed by deprotonation self-assembly of a bis-tridentate ligand consisting of two 2,6-bis-(1,2,4-triazole)-pyridine chelation arms bridged by a dibenzofuran chromophore, of which the luminescent Eu₂L₂ macrocycle can be used for enantiomeric excess (ee) detection toward pybox-type chiral ligands and selective colorimetric sensing of omethoate (OMA) in water.

Coordination-directed self-assembly has become a well-established technique for the construction of multi-functional supramolecular structures.¹ Various supramolecular complexes based on transition metals have been designed and reported.² However, research on the controllable self-assembly of lanthanide supramolecular complexes has clearly lagged behind due to the difficulty in predicting the coordination number and geometry of lanthanide elements.³ Because of the shielded 4f electrons, lanthanides have unique photophysical properties, including distinct well-defined emission bands, long lifetimes, and large Stokes shifts, and thus are widely used in phosphors, light-emitting diodes, biosensors/probes, *etc.*⁴ Direct excitation of lanthanide ions is very difficult due to the small molar extinction coefficient ($<10^{-1} \text{ M}^{-1} \text{ cm}^{-1}$) that stems from the forbidden f–f transitions.⁵ Nonetheless, strongly luminescent lanthanide–organic complexes can be obtained using suitable ligands containing suitable chromophores to sensitize the lanthanide ions through the so-called

“antenna effect”.⁶ The binding affinity of the chelating moieties, the light absorption ability and the energy level of the ligand, along with the coordination environment of the lanthanide centres, determine the stability and the sensitized luminescence performance of the final lanthanide complexes. Therefore, for the development of photo-functional lanthanide assemblies, it is critical to design appropriate ligand skeletons, especially those with new chelating groups.

Previously, many lanthanide-directed coordination assemblies from ligands with pyridine-2,6-dicarboxamide (pcam) as the chelation arms have been successively constructed.⁷ However, most of these complexes tend to dissociate in aqueous solutions and suffer from low photoluminescence quantum yields (Φ). From 2015, we have been focusing on the design of bright luminescent supramolecular lanthanide compounds. Apart from the pcam-based ligands, new ligands based on (1,2,3)-triazole-pyridine-amido (trpa), (1,2,3)-triazole-pyridine-(1,2,3)-triazole (trptr), and pyridine-2,6-bitetrazole (pbtz) chelating moieties have been successfully developed, and they showed much enhanced sensitization efficiency toward various lanthanide elements, including those emitting in the near-infrared region.⁸

Deprotonation self-assembly has been proved to be effective in constructing water-stable supramolecular coordination complexes.⁹ Very recently, we have reported a series of water-stable anionic lanthanide organic polyhedral complexes by utilizing the deprotonation self-assembly of pbtz-based ligands, which show good stability under aqueous conditions and high luminescence quantum yield ($\Phi_{\text{max}} = 11\%$ in water for the Tb cube).^{8d} These precedents motivate us to further design new ligand skeletons based on the idea of deprotonation self-assembly. While pyridine-2,6-bis-(1,2,4-triazole) (pbtr) chelates have been known for a long time, previous studies mainly focused on the complexes fabricated by transition metals, such as Fe, Pd, Pt, *etc.*¹⁰ Lanthanide complexes with pbtr-type ligands have been extremely rare reported. As far as we know, the only one-type example is [LnL(NO₃)_n] mononuclear complex, obtained by searching from the CCDC database.¹¹

^aState Key Laboratory of Structural Chemistry, Fujian Institute of Research on the Structure of Matter, Chinese Academy of Sciences, Fuzhou 350002, PR China. E-mail: qfsun@fjirsm.ac.cn

^bUniversity of Chinese Academy of Sciences, Beijing 100049, PR China

^cInstitute of Environmental Research at Greater Bay Area; Key Laboratory for Water Quality and Conservation of the Pearl River Delta, Ministry of Education; Guangzhou Key Laboratory for Clean Energy and Materials; Guangzhou University, Guangzhou 510006, China

†Electronic supplementary information (ESI) available: Experimental details, supporting figures and tables. CCDC 2065023. For ESI and crystallographic data in CIF or other electronic format see DOI: 10.1039/d1dt00726b

Particularly, with regard to our previous finding that supramolecular tetrahedra constructed with ligands based on trprtr-type chelation arms showed excellent luminescence properties ($\Phi_{\text{max}} = 82\%$ in acetonitrile for the Tb tetrahedra),^{8c} we anticipate that the replacement of (1,2,3)-triazole with 1,2,4-triazole may lead to the design of new water-stable supramolecular lanthanide complexes with bright luminescence *via* the deprotonation assembly process.

Herein, we designed a new bis-tridentate ligand (**H₄L**) consisting of two 2,6-bis-(1,2,4-triazole)-pyridine chelation arms bridged by a dibenzofuran chromophore, and studied its deprotonation self-assembly with Ln^{III} (Ln^{III} = La^{III} and Eu^{III}) ions, by which water-stable and bright luminescent Eu₂L₂ macrocycles have been obtained (Scheme 1). With available open metal sites on the Ln^{III} centres, Eu₂L₂ can further carry out post-synthetic modification with additional chiral auxiliary ligands and becomes chiroptically-active, realizing a linear ee detection through induced CD and CPL. Furthermore, the selective turn-off sensing of OMA has also been demonstrated in water, with a naked-eye recognizable color change.

As a model compound, lanthanide coordination behaviour of the tridentate ligand 4-bromo-2,6-bis(3-(trifluoromethyl)-1*H*-1,2,4-triazol-5-yl)pyridine (**H₂L'**) had been first studied. While NMR titration of Eu(OTf)₃ (0–0.5 eq.) with **H₂L'** in the presence of triethylamine (2.0 eq.) in CD₃CN indicated the formation of the 1 : 3 complexes (Fig. S13 and S14[†]), crystallization under different M/L ratios all led to the formation of a EuL'₂ complex, suggesting that EuL'₂ is a favourable thermodynamic product with this chelate. The C₂-symmetric ligand (**H₄L**) was then synthesized through the Sonogashira coupling reaction of **H₂L'** and 2,8-dialkynyl-dibenzofuran (see the Experimental section in the ESI[†] for details). Treatment of the ligand (**H₄L**) and trimethylamine (4.0 eq.) with an equimolar amount of La(OTf)₃ in dimethyl sulfoxide led to the quantitative formation of a highly symmetric product, which was confirmed by ¹H, ¹⁹F, and DOSY NMR spectra (Fig. 1B and C S16[†]). Compared with the free ligand,

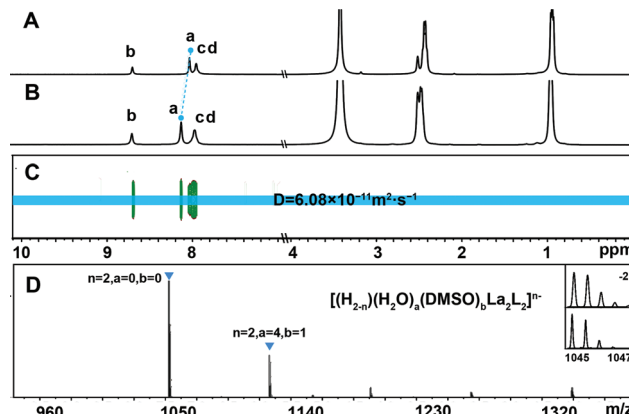
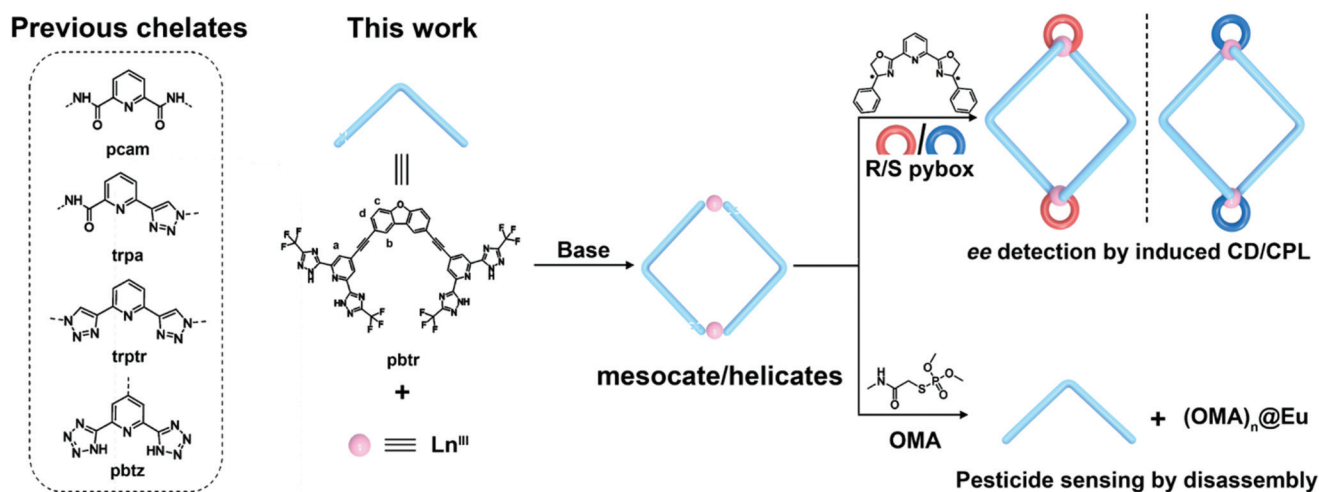


Fig. 1 ¹H NMR spectra (400 MHz, DMSO-*d*₆, 298 K) of (A) **H₄L** with Et₃N and (B) **La₂L₂**; ¹H DOSY spectrum of (C) **La₂L₂**; ESI-MS spectra of (D) **La₂L₂**.

H_a on the pyridine shifted to the lower field, while **H_{b–d}** on the dibenzofuran showed only very small shifts in the ¹H NMR after coordination to the metal. Similarly, the ¹⁹F signals also showed small movements, as the CF₃ groups are far from the metal centres (Fig. S17[†]). DOSY also indicated the formation of a single species in solution with $D = 6.08 \times 10^{-11} \text{ m}^2 \text{ s}^{-1}$. ESI-MS unambiguously confirmed a formula of **La₂L₂** for the assembly with prominent peaks observed at $m/z = 1044.9373$ and 1119.9172 , corresponding to $[\text{La}_2\text{L}_2]^{2-}$ and $[\text{La}_2\text{L}_2(\text{H}_2\text{O})_4(\text{DMSO})]^{2-}$ (Fig. 1D). Similarly, **Eu₂L₂** was synthesized by simply replacing La(OTf)₃ with Eu(OTf)₃, and its structure was determined by ESI-TOF-MS (Fig. S75 and Table S1[†]).

The single-crystal X-ray structure of the europium mononuclear complex **EuL'₂** is shown in Fig. 2A. The crystallographic data showed that the Eu^{III} ions are nine coordinated by two bis(1,2,4-triazole) chelating groups and three additional water molecules (Fig. 2B). The mean distance from the metal centre to the nitrogen atom on pyridine is 2.69 Å, and the



Scheme 1 Self-assembly of water-stable macrocycles for ee detection and OMA sensing.

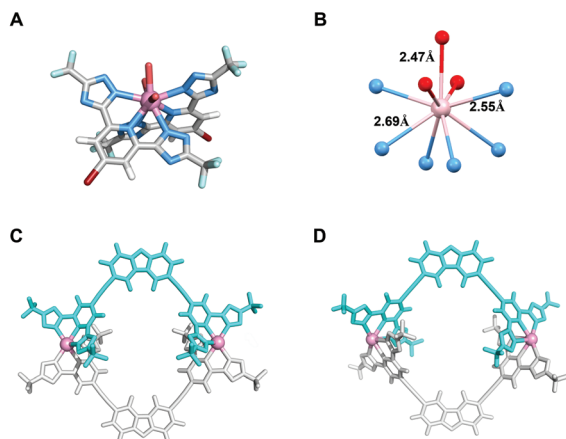


Fig. 2 X-ray crystal structure (A) of Eu_2L_2 (color code for Eu: pink sphere, C: gray, N: light blue, Br: dark red, F: cyan, H: white, and O: orange) and (B) the local coordination environment of the Eu centre; energy-minimized structures of a mesocate (C) and a $\Lambda\Lambda$ -helicate (D) for the Eu_2L_2 complex.

mean distance to the nitrogen atom on 1,2,4-triazole is 2.55 Å, which are slightly shorter than those of the trptr system (2.60 Å and 2.56 Å) and longer than those of the pbtz system (2.56 Å and 2.43 Å).^{8c,d} In addition, the mean distance between the metal centre and the coordinating H_2O is 2.47 Å. The dihedral angle of two bis (1,2,4-triazole) chelating groups is 80.16°. Potentially due to the fact that both mesocate (Λ,Δ) and racemic mixtures of helicates (Λ,Λ and Δ,Δ) are the possible outcomes for the M_2L_2 complex, attempts to crystallize the Ln_2L_2 complex were unsuccessful, and so their structures were simulated by molecular mechanic modelling. In the case of a mesocate structure (Fig. 2C), the pyridine ring and the 1,2,4-triazole ring are distorted from the planar geometry due to steric hindrance, which has also been found in the previously reported crystal structures.¹² The two ligands are in an antiparallel geometry and the whole structure is C_{2v} symmetric. On the other hand, in the optimized helicate structure (Fig. 2D), the pyridine rings and the two 1,2,4-triazole rings are planar. The two ligand chains adopted a crossover chelation geometry toward the two lanthanide centres, where the chirality on the two metal centres is consistent (Λ,Λ or Δ,Δ), giving rise to a whole D_2 symmetry of the helicate.

The photophysical parameters of **L** and Eu_2L_2 are summarized in Table 1. In DMSO, the UV-vis absorption of the Eu_2L_2

Table 1 Photophysical data for the ligand and macrocycles

Complex	λ_{ex} [nm]	$\lambda_{\text{em}}^{\text{max}}$ [nm]	τ_{obs}	Φ_{overall}
Eu_2L_2^a	333	616	1.9 ms	69.31%
L ^b	324	438	15.2 ns	6.05%
Eu_2L_2^c	335	612	1.6 ms	55.66%
Eu_2L_2^b	336	615	320.0 μs	4.21%
$\text{Eu}_2\text{L}_2\text{A}^{\text{S}_2}$ ^c	335	615	3.2 ms	75.05%

^a In DMSO. ^b In H_2O . ^c In CH_3CN .

macrocycle between 300 and 350 nm decreased and the absorption between 250 and 275 nm increased compared to the deprotonated ligand (Fig. S22†). Upon excitation at 333 nm, the characteristic red emission peaks of Eu^{III} were observed at 591, 616, 688, and 692 nm, corresponding to the $^5\text{D}_0 \rightarrow ^7\text{F}_J$ ($J = 1-4$) transitions respectively (Fig. S25†). Surprisingly, the quantum yield of Eu_2L_2 is as high as 69.31% at room temperature (Fig. S29†). The luminescence lifetime of the $^5\text{D}_0$ excited state was 1.9 ms (Fig. S32†). However, the quantum yield and lifetime in CH_3CN decreased to 55.66% and 1.6 ms, respectively (Fig. S43 and S46†). Impressively, Eu_2L_2 is found to be stable in water, as the characteristic red luminescence still remained after diluting its DMSO solution in H_2O , even after 45 days. The luminescence spectrum showed that the emission quantum yield was as high as 4.21% in H_2O (Fig. S31†). The number of solvent molecules coordinated to the Eu^{III} ions in the first coordination sphere (q) for Eu_2L_2 was then determined to be 2.9 by measuring the corresponding luminescence lifetimes in both H_2O and D_2O (see ESI† for details), suggesting that the structure of Eu_2L_2 did not change. ESI-TOF-MS also proved that the structure of Eu_2L_2 is maintained in H_2O (Fig. S76†).

Considering that the Eu_2L_2 has unsaturated metal centres, addition of chiral ancillary ligands may induce CD and CPL responses *via* the post-synthetic modification mechanism.¹³ Indeed, titration of 2,6-bis(4-phenyl-2-oxazolonyl)pyridine (pybox, A^{R} and A^{S}) with varying ee compositions into Eu_2L_2 led to gradually changing ICD signals in CH_3CN . Perfect mirror images of CDs in the 250–400 nm range induced by adding the opposite ee values of pybox were observed and a linear relationship was confirmed between the CD responses at 310 and 345 nm and the ee values (Fig. 3A and C). Similarly, while Eu_2L_2 is CPL silent, perfect linear responses of ICPL signals against the ee values were observed at 597, 611.5, and 695.5 nm (Fig. 3B and D) in the presence of the pybox ligands with varying enantiomeric compositions. Chelation of the pybox onto Eu_2L_2 has been confirmed by ESI-TOF-MS, with prominent peaks observed at $m/z = 1428.1371$ and 1535.1572 , corresponding to $[\text{Eu}_2\text{L}_2\text{A}^{\text{S}_2}]^{2-}$ and $[\text{Eu}_2\text{L}_2\text{A}^{\text{S}_2}(\text{CH}_3\text{CN})_2(\text{H}_2\text{O})_3(\text{DMSO})]^{2-}$ (Fig. S77†). Moreover, the emission intensity of $\text{Eu}_2\text{L}_2\text{A}^{\text{S}_2}$ was obviously enhanced compared to Eu_2L_2 , whereas the photoluminescence quantum yields increased from 55.66% to 74.57%, and the lifetimes also increased from 1.6 to 3.2 ms (Fig. S45 and S47†). The emission enhancement can be attributed to the replacement of the coordination solvent molecules with the auxiliary ligands, which effectively inhibits the non-radiative inactivity of the europium ions. The structures of $\text{Eu}_2\text{L}_2\text{A}^{\text{R}_2}$ and $\text{Eu}_2\text{L}_2\text{A}^{\text{S}_2}$ were simulated by molecular modelling, where the strong π - π stacking interactions between the side phenyl rings of pybox and the pyridyl ring of ligand **L** are indicated (Fig. 3E and F).

Omethoate (OMA) is a priority monitoring hazardous substrate in pesticides due to its high toxicity to organisms and humans.¹⁴ An effective method to monitor and detect low doses of OMA in water is important as it is being used worldwide as acaricide and insecticide in the agricultural field.¹⁵ Considering that Eu_2L_2 is stable in water, the sensing toward common pesti-

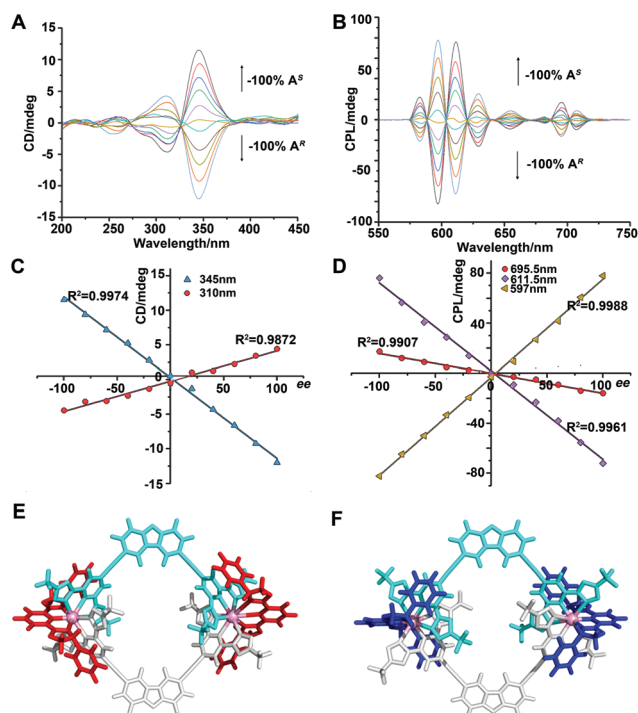


Fig. 3 (A) CD spectra of Eu_2L_2 (5×10^{-6} M, CH_3CN) containing 2 eq. of $\text{A}^{\text{R/S}}$ with various ee values, and (C) the corresponding ee calibration plots at 310 nm and 345 nm. (B) CPL spectra of Eu_2L_2 (2×10^{-5} M, CH_3CN) containing 2 eq. of $\text{A}^{\text{R/S}}$ with various ee values, and (D) the corresponding ee calibration plots at 597, 611.5, and 695.5 nm. Energy-minimized structures of $\text{Eu}_2\text{L}_2\text{A}^{\text{R}}_2$ (E) and $\text{Eu}_2\text{L}_2\text{A}^{\text{S}}_2$ (F).

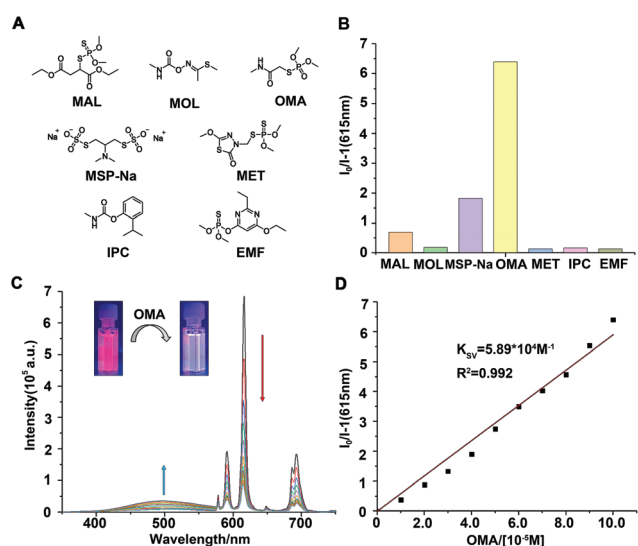


Fig. 4 (A) Chemical structures of different pesticides. (B) Luminescence response of Eu_2L_2 to various pesticides (10 eq.). (C) Luminescence titration spectra of Eu_2L_2 (1.0×10^{-5} M) containing different equivalents of OMA in H_2O . (D) The fitting plot of $I_0/I - 1$ at 615 nm versus the equivalents of OMA.

cides (Fig. 4A), including malathion (MAL), methomyl (MOL), molosultap (MSP-Na), omethoate (OMA), methidathion (MET), isoprocarb (IPC), and etrimfos (EMF) was then screened

(Fig. S49–63[†]). Surprisingly, with the addition of 10.0 eq. of different analytes to the aqueous solution of Eu_2L_2 , only OMA led to significant luminescence quenching (Fig. 4B), while no such significant responses have been observed for all the other pesticides. Under UV irradiation at 365 nm, the luminescence of the solution changes from pink to yellow-green after the addition of OMA, which is easily recognizable by the naked eye (Fig. 4C). Titration of OMA (1–10 eq.) into Eu_2L_2 confirmed a good linear relationship between the I_0/I ratio at 615 nm and the equivalents of OMA, with a detection limit as low as 9 nM being estimated ($S/N = 3$) (Fig. 4D and S65[†]). Based on the emergence of a broad-band emission at 500 nm and the observation of m/z signals assigned to H_2L^{2-} , $[\text{Eu}@(\text{OMA})_2]^{3+}$ and $[\text{Eu}@(\text{OMA})_3]^{2+}$ in the ESI-TOF-MS spectra (Fig. S78 and S79[†]) after the titration, a disassembly mechanism was accounted for this colorimetric sensing.

Conclusions

In summary, water-stable anionic lanthanide-organic macrocycles have been constructed by coordination-driven self-assembly of a new bis-tridentate 1,2,4-triazole-based ligand with Ln^{III} metals. Eu_2L_2 exhibits unparalleled photoluminescence quantum yields in DMSO/water and can be used for ee detection and selective OMA sensing. Our results offer new candidates for the ligand design toward water-stable multi-functional lanthanide-organic architectures.

Conflicts of interest

There are no conflicts to declare.

Acknowledgements

This work was supported by the NSFC (Grant No. 21825107) and the Strategic Priority Research Program of the Chinese Academy of Sciences (Grant No. XDB20000000).

Notes and references

- (a) M. Fujita, M. Tominaga, A. Hori and B. Therrien, *Acc. Chem. Res.*, 2005, **38**, 369–378; (b) W. X. Gao, H. J. Feng, B. B. Guo, Y. Lu and G. X. Jin, *Chem. Rev.*, 2020, **120**, 6288–6325; (c) A. J. McConnell, C. S. Wood, P. P. Neelakandan and J. R. Nitschke, *Chem. Rev.*, 2015, **115**, 7729–7793; (d) Y. Sun, C. Chen, J. Liu and P. J. Stang, *Chem. Soc. Rev.*, 2020, **49**, 3889–3919; (e) W. Wang, Y. X. Wang and H. B. Yang, *Chem. Soc. Rev.*, 2016, **45**, 2656–2693.
- (a) C. Ngai, C. M. Sanchez-Marsetti, W. H. Harman and R. J. Hooley, *Angew. Chem., Int. Ed.*, 2020, **59**, 23505–23509; (b) H. Wang, L. P. Zhou, Y. Zheng, K. Wang, B. Song, X. Yan, L. Wojtas, X. Q. Wang, X. Jiang, M. Wang, Q. F. Sun, B. Xu, H. B. Yang, A. C. Sue, Y. T. Chan, J. L. Sessler, Y. Jiao,

- P. J. Stang and X. Li, *Angew. Chem., Int. Ed.*, 2021, **60**, 1298–1305; (c) Z. Wang, C. Y. Zhu, J. T. Mo, X. Y. Xu, J. Ruan, M. Pan and C. Y. Su, *Angew. Chem., Int. Ed.*, 2021, **60**, 2526–2533; (d) J. H. Zhang, H. P. Wang, L. Y. Zhang, S. C. Wei, Z. W. Wei, M. Pan and C. Y. Su, *Chem. Sci.*, 2020, **11**, 8885–8894; (e) G. Liu, Z. Ju, D. Yuan and M. Hong, *Inorg. Chem.*, 2013, **52**, 13815–13817; (f) S. M. Bierschenk, R. G. Bergman, K. N. Raymond and F. D. Toste, *J. Am. Chem. Soc.*, 2020, **142**, 733–737; (g) P. Howlader, S. Mondal, S. Ahmed and P. S. Mukherjee, *J. Am. Chem. Soc.*, 2020, **142**, 20968–20972; (h) P. Howlader, E. Zangrando and P. S. Mukherjee, *J. Am. Chem. Soc.*, 2020, **142**, 9070–9078; (i) M. Wang, C. Wang, X. Q. Hao, J. Liu, X. Li, C. Xu, A. Lopez, L. Sun, M. P. Song, H. B. Yang and X. Li, *J. Am. Chem. Soc.*, 2014, **136**, 6664–6671; (j) T. Z. Xie, K. J. Endres, Z. Guo, J. M. Ludlow, 3rd, C. N. Moorefield, M. J. Saunders, C. Wesdemiotis and G. R. Newkome, *J. Am. Chem. Soc.*, 2016, **138**, 12344–12347; (k) J. Jiao, Z. Li, Z. Qiao, X. Li, Y. Liu, J. Dong, J. Jiang and Y. Cui, *Nat. Commun.*, 2018, **9**, 4423; (l) T. Z. Xie, Y. Yao, X. Sun, K. J. Endres, S. Zhu, X. Wu, H. Li, J. M. Ludlow III, T. Liu, M. Gao, C. N. Moorefield, M. J. Saunders, C. Wesdemiotis and G. R. Newkome, *Dalton Trans.*, 2018, **47**, 7528–7533; (m) L. J. Chen and H. B. Yang, *Acc. Chem. Res.*, 2018, **51**, 2699–2710; (n) M. Li, L.-J. Chen, Y. Cai, Q. Luo, W. Li, H.-B. Yang, H. Tian and W.-H. Zhu, *Chem*, 2019, **5**, 634–648; (o) W. Zheng, W. Wang, S. T. Jiang, G. Yang, Z. Li, X. Q. Wang, G. Q. Yin, Y. Zhang, H. Tan, X. Li, H. Ding, G. Chen and H. B. Yang, *J. Am. Chem. Soc.*, 2019, **141**, 583–591.
- 3 (a) B. Wang, Z. Zang, H. Wang, W. Dou, X. Tang, W. Liu, Y. Shao, J. Ma, Y. Li and J. Zhou, *Angew. Chem., Int. Ed.*, 2013, **52**, 3756–3759; (b) A. M. Johnson, C. A. Wiley, M. C. Young, X. Zhang, Y. Lyon, R. R. Julian and R. J. Hooley, *Angew. Chem., Int. Ed.*, 2015, **54**, 5641–5645; (c) C. L. Liu, L. P. Zhou, D. Tripathy and Q. F. Sun, *Chem. Commun.*, 2017, **53**, 2459–2462; (d) C. L. Liu, R. L. Zhang, C. S. Lin, L. P. Zhou, L. X. Cai, J. T. Kong, S. Q. Yang, K. L. Han and Q. F. Sun, *J. Am. Chem. Soc.*, 2017, **139**, 12474–12479.
- 4 (a) P. F. Feng, M. Y. Kong, Y. W. Yang, P. R. Su, C. F. Shan, X. X. Yang, J. Cao, W. S. Liu, W. Feng and Y. Tang, *ACS Appl. Mater. Interfaces*, 2019, **11**, 1247–1253; (b) J. Yang, T. Wang, R. Guo, D. Yao, W. Guo, S. Liu, Z. Li, Y. Wang and H. Li, *ACS Appl. Mater. Interfaces*, 2020, **12**, 54026–54034; (c) T. Feng, Y. Ye, X. Liu, H. Cui, Z. Li, Y. Zhang, B. Liang, H. Li and B. Chen, *Angew. Chem., Int. Ed.*, 2020, **59**, 21752–21757; (d) M. Pan, W. M. Liao, S. Y. Yin, S. S. Sun and C. Y. Su, *Chem. Rev.*, 2018, **118**, 8889–8935; (e) J. Chen, Z. Xie, L. Meng, Z. Hu, X. Kuang, Y. Xie and C. Z. Lu, *Inorg. Chem.*, 2020, **59**, 6963–6977; (f) J. Jia, Y. Zhang, M. Zheng, C. Shan, H. Yan, W. Wu, X. Gao, B. Cheng, W. Liu and Y. Tang, *Inorg. Chem.*, 2018, **57**, 300–310; (g) X. Li, S. Lu, D. Tu, W. Zheng and X. Chen, *Nanoscale*, 2020, **12**, 15021–15035.
- 5 J. Georges, *Analyst*, 1993, **118**, 1481–1486.
- 6 (a) J. C. Bunzli and C. Piguet, *Chem. Soc. Rev.*, 2005, **34**, 1048–1077; (b) S. V. Eliseeva and J. C. Bunzli, *Chem. Soc. Rev.*, 2010, **39**, 189–227.
- 7 (a) L. S. Lisboa, J. A. Findlay, L. J. Wright, C. G. Hartinger and J. D. Crowley, *Angew. Chem., Int. Ed.*, 2020, **59**, 11101–11107; (b) T. R. Schulte, J. J. Holstein, L. Schneider, A. Adam, G. Haberhauer and G. H. Clever, *Angew. Chem., Int. Ed.*, 2020, **59**, 22489–22493; (c) X. Z. Li, L. P. Zhou, S. J. Hu, L. X. Cai, X. Q. Guo, Z. Wang and Q. F. Sun, *Chem. Commun.*, 2020, **56**, 4416–4419; (d) L. X. Cai, L. L. Yan, S. C. Li, L. P. Zhou and Q. F. Sun, *Dalton Trans.*, 2018, **47**, 14204–14210; (e) B. El Aroussi, S. Zebret, C. Besnard, P. Perrottet and J. Hamacek, *J. Am. Chem. Soc.*, 2011, **133**, 10764–10767; (f) X. Z. Li, L. P. Zhou, L. L. Yan, D. Q. Yuan, C. S. Lin and Q. F. Sun, *J. Am. Chem. Soc.*, 2017, **139**, 8237–8244; (g) F. Stomeo, C. Lincheneau, J. P. Leonard, J. E. O'Brien, R. D. Peacock, C. P. McCoy and T. Gunnlaugsson, *J. Am. Chem. Soc.*, 2009, **131**, 9636–9637; (h) L. L. Yan, C. H. Tan, G. L. Zhang, L. P. Zhou, J. C. Bunzli and Q. F. Sun, *J. Am. Chem. Soc.*, 2015, **137**, 8550–8555; (i) D. A. Leigh, J. J. Danon, S. D. P. Fielden, J. F. Lemonnier, G. F. S. Whitehead and S. L. Woltering, *Nat. Commun.*, 2021, **13**, 117–122; (j) X. Z. Li, L. P. Zhou, L. L. Yan, Y. M. Dong, Z. L. Bai, X. Q. Sun, J. Diwu, S. Wang, J. C. Bunzli and Q. F. Sun, *Nat. Commun.*, 2018, **9**, 547; (k) C.-T. Yeung, K.-H. Yim, H.-Y. Wong, R. Pal, W.-S. Lo, S.-C. Yan, M. Yee-Man Wong, D. Yufit, D. E. Smiles, L. J. McCormick, S. J. Teat, D. K. Shuh, W.-T. Wong and G.-L. Law, *Nat. Commun.*, 2017, **8**, 1128.
- 8 (a) X. Q. Guo, L. P. Zhou, L. X. Cai and Q. F. Sun, *Chem. – Eur. J.*, 2018, **24**, 6936–6940; (b) S. J. Hu, X. Q. Guo, L. P. Zhou, L. X. Cai and Q. F. Sun, *Chin. J. Chem.*, 2019, **37**, 657–662; (c) S. Y. Wu, X. Q. Guo, L. P. Zhou and Q. F. Sun, *Inorg. Chem.*, 2019, **58**, 7091–7098; (d) Z. Wang, L. He, B. Liu, L. P. Zhou, L. X. Cai, S. J. Hu, X. Z. Li, Z. Li, T. Chen, X. Li and Q. F. Sun, *J. Am. Chem. Soc.*, 2020, **142**, 16409–16419.
- 9 (a) W. Q. Sun, J. Tong, H. L. Lu, T. T. Ma, H. W. Ma and S. Y. Yu, *Chem. – Asian J.*, 2018, **13**, 1108–1113; (b) Y. P. He, L. B. Yuan, G. H. Chen, Q. P. Lin, F. Wang, L. Zhang and J. Zhang, *J. Am. Chem. Soc.*, 2017, **139**, 16845–16851; (c) E. G. Moore, J. Xu, C. J. Jocher, E. J. Werner and K. N. Raymond, *J. Am. Chem. Soc.*, 2006, **128**, 10648–10649; (d) Z. Ni, A. Yassar, T. Antoun and O. M. Yaghi, *J. Am. Chem. Soc.*, 2005, **127**, 12752–12753; (e) J. Wang, C. He, P. Wu, J. Wang and C. Duan, *J. Am. Chem. Soc.*, 2011, **133**, 12402–12405.
- 10 (a) K. Sugiyarto, D. Craig, A. Rae and H. Goodwin, *Aust. J. Chem.*, 1993, **46**, 1269–1290; (b) J. Sanning, P. R. Ewen, L. Stegemann, J. Schmidt, C. G. Daniliuc, T. Koch, N. L. Doltsinis, D. Wegner and C. A. Strassert, *Angew. Chem., Int. Ed.*, 2015, **54**, 786–791; (c) B. V. Zakharchenko, D. M. Khomenko, R. O. Doroshchuk, O. V. Severynovska, I. V. Raspertova, V. S. Starova and R. D. Lampeka, *Chem. Pap.*, 2017, **71**, 2003–2009; (d) Y. Atolini, E. A. Prasetyanto, P. Chen, S. Silvestrini, J. Harrowfield and L. De Cola, *Chem. – Eur. J.*, 2018, **24**, 12054–12060.
- 11 (a) M. G. B. Drew, M. J. Hudson, P. B. Iveson, C. Madic and M. L. Russell, *J. Chem. Soc., Dalton Trans.*, 1999, **1**, 2433–

- 2440; (b) Z. Xu, X. He, Y. He, X. Zhao, M. Batmunkh, H. Li, Y. Wang, J. Cao and T. Ma, *Talanta*, 2020, **208**, 120363.
- 12 Q. Y. Zhu, L. P. Zhou and Q. F. Sun, *Dalton Trans.*, 2019, **48**, 4479–4483.
- 13 (a) Q. Y. Zhu, L. P. Zhou, L. X. Cai, X. Z. Li, J. Zhou and Q. F. Sun, *Chem. Commun.*, 2020, **56**, 2861–2864; (b) Z. Wang and S. M. Cohen, *Chem. Soc. Rev.*, 2009, **38**, 1315–1329.
- 14 (a) B. Pina-Guzman, M. Sanchez-Gutierrez, F. Marchetti, I. Hernandez-Ochoa, M. J. Solis-Heredia and B. Quintanilla-Vega, *Toxicol. Appl. Pharmacol.*, 2009, **238**, 141–149; (b) C. C. Lerro, S. Koutros, G. Andreotti, M. C. Friesen, M. C. Alavanja, A. Blair, J. A. Hoppin, D. P. Sandler, J. H. Lubin, X. Ma, Y. Zhang and L. E. Beane Freeman, *Occup. Environ. Med.*, 2015, **72**, 736–744.
- 15 D. Huo, S. Jiang, Z. Qin, Y. Feng, R. Yang, L. Lv and Y. Li, *Toxicology*, 2019, **427**, 152298.